Temperature-Induced Increase of Spin Spiral Periods

Aurore Finco,[1,*] Levente Rózsa,[1,2] Pin-Jui Hsu,[1] André Kubetzka,[1] Elena Vedmedenko,[1]
Kirsten von Bergmann,[1] and Roland Wiesendanger[1]

[1]*Department of Physics, University of Hamburg, D-20355 Hamburg, Germany*
[2]*Institute for Solid State Physics and Optics, Wigner Research Centre for Physics, Hungarian Academy of Sciences,*
P.O. Box 49, H-1525 Budapest, Hungary

Spin-polarized scanning tunneling microscopy investigations reveal a significant increase of the magnetic period of spin spirals in three-atomic-layer-thick Fe films on Ir(111), from about 4 nm at 8 K to about 65 nm at room temperature. We attribute this considerable influence of temperature on the magnetic length scale of noncollinear spin states to different exchange interaction coefficients in the different Fe layers. We thus propose a classical spin model that reproduces the experimental observations and in which the crucial feature is the presence of magnetically coupled atomic layers with different interaction strengths. This model might also apply for many other systems, especially magnetic multilayers.

Recently, significant attention has turned towards the possible spintronics applications of noncollinear magnetic configurations in ultrathin films, including chiral domain walls [1] and isolated Skyrmions [2]. The Dzyaloshinsky-Moriya interaction [3,4], induced by the breaking of inversion symmetry at the interface and the strong spin-orbit coupling in the substrate, plays an important role in stabilizing such noncollinear states. Crucial points for improving spintronics devices do not only include decreasing the electrical currents and magnetic fields necessary for their operation, but also ensuring a good thermal stability. A possible solution to the latter problem is to use magnetic films or multilayers with a thickness such that the critical temperature is well above 300 K, which has been proven successful in stabilizing room-temperature Skyrmions [5–8]. Here, we aim to improve thermal stability in simple epitaxial systems by increasing the thickness of an Fe layer on Ir(111), where the Fe/Ir interface is known to induce a strong Dzyaloshinsky-Moriya interaction [9]. Spin-polarized scanning tunneling microscopy (SP-STM) measurements revealed a nano-Skyrmion lattice in the monolayer Fe on Ir (111), which vanishes at 28 K [10]. Since it was predicted and observed for various transition metal ultrathin films that the Curie temperature increases with the thickness of the film [11–13], we expect an improved thermal stability for the double- and triple-layer Fe films.

In the monolayer, the experiments did not reveal a modification of the ratio between the atomic and magnetic periods with the increase in temperature [10], which is also the case for other noncollinear spin states at the nanometer scale, for example, in the monolayer Mn [14] and the double layer Fe on W(110) [15]. However, in several bulk materials it has already been observed [16] that the period of the noncollinear order within the incommensurate phase may depend on the temperature. For example, the period gradually increases with temperature by less than 10% in $USb_{0.9}Te_{0.1}$

[17], while it decreases by about 30% in Dy and Er [16]. In some cases, the change in the magnetic period is connected to a similar modification of the atomic structure with temperature, as was demonstrated in bulk $ZnCr_2Se_4$ [18].

In this Letter, we report on SP-STM measurements performed on ultrathin Fe films on Ir(111) at various temperatures. We demonstrate that the critical temperature of the noncollinear order significantly rises from 28 K in the monolayer [10] through 150–200 K in the double layer to above room temperature in the triple layer. Furthermore, we show that the period of the cycloidal spin spiral state gradually increases from 4 nm at 8 K to about 65 nm at room temperature in the triple layer. Although an enhancement of the period with temperature is not unprecedented [16], its magnitude is remarkably large in the present system. We attribute this trend to the different strain relief and hybridization effects between the three atomic layers, and construct a classical spin model with layer-dependent interaction parameters to explain the phenomenon. For ultrathin films thicker than a monolayer, an effective model with a mapping onto a single layer might be too simplistic to describe the influence of temperature on the spin structure. This could be important, e.g., in the calculation of magnetic phase diagrams, especially for multilayer systems with many different interfaces.

The SP-STM measurements performed at different temperatures are illustrated in Fig. 1. The experimental methods are discussed in the Supplemental Material [19]. Because of the large lattice mismatch between the Fe layer and the Ir substrate, the films exhibit dislocation lines for coverages above a monolayer [26–28] as visible in the constant-current topography image in Fig. 1(a). The noncollinear magnetic structure of the Fe film at low temperature is visible in the spin-polarized differential conductance map in Fig. 1(b) showing the out-of-plane component of the sample magnetization. The alternating bright and dark stripes correspond
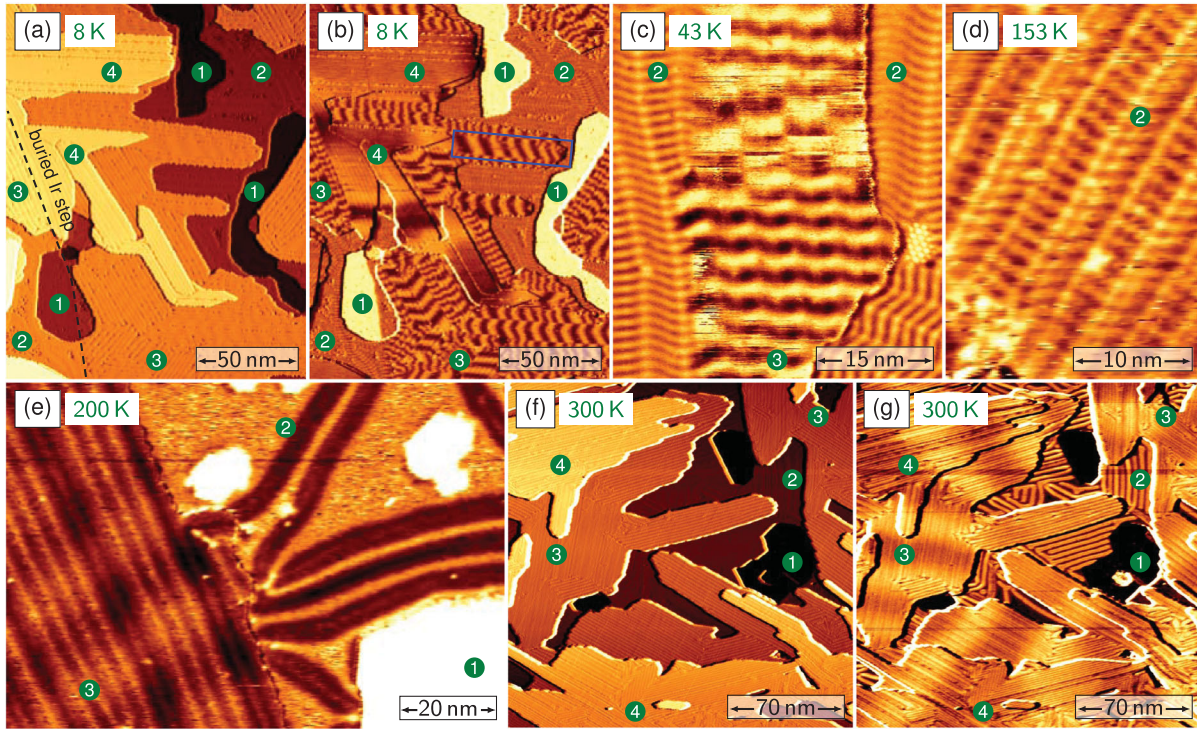
FIG. 1.   STM constant-current topography [(a),(f)] and spin-polarized differential conductance maps [(b)–(e),(g)] of ultrathin Fe films on Ir(111) for double-, triple-, and quadruple-layer coverages (indicated by the green circles). The simultaneously recorded current map was added to the constant-current topography in (a) and (f) to enhance the visibility of the dislocation lines. The spin spirals in the double layer are not visible at 200 K anymore in (e), and the contrast visible in (g) in the double-layer regions is created by the dislocation lines. The spin spiral period in the triple layer gradually increases from 4 nm in (b) to 65 nm in (g). The quadruple layer is ferromagnetic in (b), whereas it forms a continuous spin spiral state with the triple layer in (g). The measurements shown in panels (a) and (b) and panels (f) and (g) were performed with an out-of-plane-sensitive antiferromagnetic Cr bulk tip, and the ones in panels (c)–(e) were performed with a ferromagnetic Fe coated W tip. Measurement parameters: (a),(b) $U = -700$ mV, $I = 1$ nA, (c) $U = -700$ mV, $I = 0.6$ nA, (d) $U = -500$ mV, $I = 2$ nA, (e) $U = -700$ mV, $I = 2$ nA, (f),(g) $U = -500$ mV, $I = 3$ nA.

to cycloidal spin spirals propagating along the dislocation lines in both the double- and triple-layer areas. The distance between these lines is locally varying, because the strain relief is not uniform. The period of the spin spirals is correlated with the strain variation, which induces a spreading of the wavelengths between 1.5 and 2 nm in the double layer [26]. Furthermore, two types of dislocation lines coexist in the triple layer. In one case, the spin spirals have a period of 3 to 4 nm and a zigzag-shaped wave front [clearly visible in Fig. 1(c)], whereas on the other type of area the periods are ranging from 5 to 10 nm and the wave front is straight but canted with respect to the dislocation lines [see the blue box in Fig. 1(b)]. These differences arise from the local arrangement of the atoms in the Fe layer [28]. In addition to previous reports, the magnetic state of the quadruple layer is also shown in the image. It is ferromagnetic at low temperature on the length scale of the island size (about 100 nm), with the domains assuming several different magnetization directions, which we attribute to a weak magnetic anisotropy.

The temperature was raised in several steps up to room temperature. Up to 150 K, the wave front shape of the spin

spirals is conserved in the double layer and their period stays within the range observed at low temperature, see Figs. 1(c) and 1(d). A possible increase of the wavelength with temperature is too small to be distinguished from the strain-induced variations. The magnetic contrast vanishes between 150 and 200 K in the double layer [cf. Figs. 1(d) and 1(e)], which demonstrates the enhancement of the thermal stability over the monolayer case where the nano-Skyrmion lattice disappears at 28 K [10]. However, since our SP-STM measurements are time averaged, this vanishing could be caused by spin fluctuations within a shorter time scale than the measurement and thus the actual critical temperature for the double layer might be higher [29].

In the triple layer, the period of the spin spirals increases clearly and at 200 K, the spiral wave fronts are not zigzag shaped anymore, with a wavelength of 14 nm in the area shown in Fig. 1(e). At room temperature, the magnetism looks strikingly different from the low-temperature case as illustrated in Fig. 1(g). The spiral wavelengths are much larger (between 55 and 80 nm) and all the wave fronts are straight and perpendicular to the dislocation lines. Note that the spirals are nevertheless still guided by the dislocation

lines, but the local atomic arrangement does not influence the wave front anymore for such large magnetic length scales. Furthermore, the spirals cross the step edges between the triple- and quadruple-layer Fe areas, highlighting a ferromagnetic coupling between the third and the fourth atomic layers, which exhibit the same magnetic wavelength.

In order to quantify the period increase in the triple layer, further measurements were performed at intermediate temperatures and the data are collected in Fig. 2(a). On
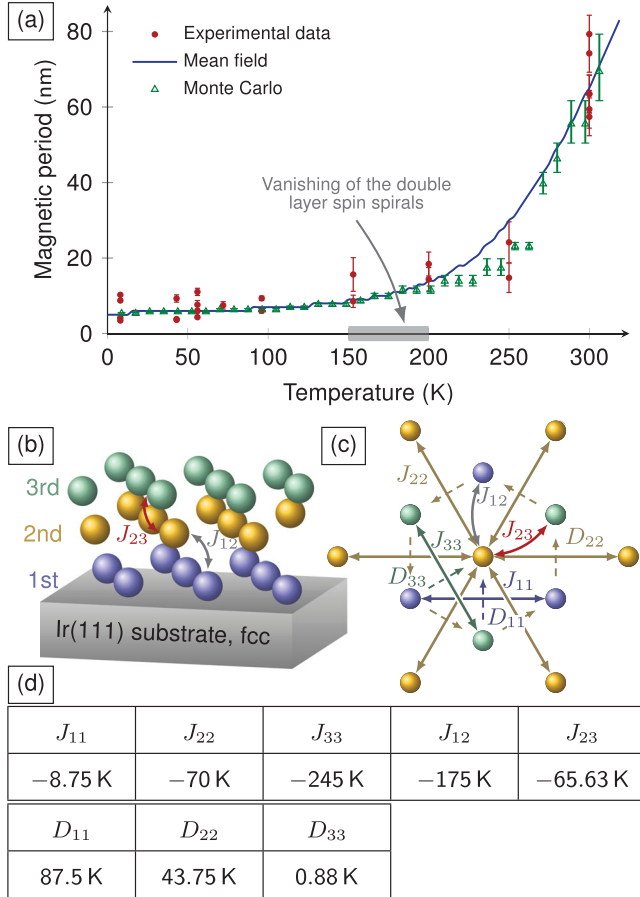

FIG. 2. (a) Magnetic period of the spin spirals in the triple-layer Fe on Ir(111) at different temperatures from experiments, mean-field calculations, and Monte Carlo simulations. The temperature scale for the mean-field data was rescaled by a factor of 0.71 for better comparison, since it significantly overestimates the temperature range of the period change as well as the critical temperature. The error bars reflect the resolution of the Fourier transformation (used to measure the period from the experimental data and from the simulations) as well as the thermal drift in the experiment. (b),(c) Schematic view of the model system used to describe the triple-layer Fe on Ir(111) in the theoretical calculations, with the coupling constants used in Eq. (1). Perfect fcc stacking was used to simplify the geometry of the model. The intralayer couplings are different in every layer, with $|J_{11}| < |J_{22}| < |J_{33}|$ for the Heisenberg couplings and $D_{11} > D_{22} > D_{33}$ for the Dzyaloshinsky-Moriya interactions. (d) Numerical values of the coupling constants used for the Monte Carlo simulations in (a), with the notations of (b) and (c).

average, the period rises by a factor of 4 between 8 and 250 K, and again by a factor of 4 between 250 K and room temperature. The large dispersion of the data points at each temperature is linked to the strain-relief effect discussed in Ref. [28].

For a quantitative theoretical explanation of the remarkable increase of the spiral wavelength with temperature, we relied on a model that treats the three atomic layers of Fe separately instead of using single Heisenberg and Dzyaloshinsky-Moriya interactions for the whole ultrathin film. The model Hamiltonian reads

$$H = \frac{1}{2} \sum_{p,q,\langle i,j \rangle} J_{pq,ij} \mathbf{S}_{p,i} \mathbf{S}_{q,j} + \frac{1}{2} \sum_{p,\langle i,j \rangle} \mathbf{D}_{pp,ij} (\mathbf{S}_{p,i} \times \mathbf{S}_{p,j}), \quad (1)$$

also illustrated in Figs. 2(b) and 2(c). $\mathbf{S}_{p,i}$ denote classical unit vectors representing the magnetic moments. The p, $q = 1, 2, 3$ indices denote the three layers starting from the one closest to the Ir substrate, while i and j are intralayer indices. The summations only run over the nearest neighbors, including six intralayer neighbors and three neighbors in each adjacent layer.

The $J_{pq,ij}$ coefficients denote intralayer and interlayer Heisenberg exchange interactions. The intralayer Dzyaloshinsky-Moriya vectors $\mathbf{D}_{pp,ij}$ are perpendicular to the nearest-neighbor bonds and are chosen to be in plane—see the dashed arrows in Fig. 2(c).

Regarding the temperature-dependent spin spiral period, the crucial point about Eq. (1) is the consideration of layer-dependent interaction parameters. Layer-dependent coupling coefficients naturally appear during *ab initio* calculations [30–33] due to the different hybridization effects for atomic layers with different distances to the nonmagnetic substrate and the vacuum interface. In the present system, this choice is further supported by the fact that the actual intralayer atomic distances may differ between the three Fe layers due to the strain relief [27,28]. Note that the microscopic parameters in Eq. (1) are not explicitly temperature dependent. In an atomistic model this is generally justified for Fe, which has strong localized magnetic moments [34]. In principle, a modification of the atomic structure with temperature could influence the coupling coefficients [18,35]. However, we did not observe any obvious modification of the structure of the Fe film as a function of temperature in the topographic images. In addition, the mechanisms discussed in Ref. [16] for homogeneous bulk magnets seemed to be insufficient to quantitatively explain the exceptionally large increase of the period in the triple layer Fe.

For obtaining such a strong temperature dependence of the period, it was necessary to assume that the J_{pp} and $\mathbf{D}_{pp}$ intralayer couplings determine different spiral periods in the different layers. The Dzyaloshinsky-Moriya interaction is expected to get weaker when moving away from the Ir substrate, since it primarily appears at the interface between

the magnetic Fe layers and the heavy metal Ir substrate with strong spin-orbit coupling. On the contrary, it is assumed that the Heisenberg exchange interactions get stronger when moving away from the substrate. It was demonstrated in Ref. [28] that the spin spiral period at a fixed temperature is locally larger where the Fe atoms in the reconstructed third layer are closer to each other, indicating an increase of the Heisenberg exchange interactions as the atoms rearrange into a bulklike bcc structure. Furthermore, earlier *ab initio* calculations indicated a weakening of the Heisenberg exchange interactions at Fe/Ir interfaces due to hybridization effects [36–39]. As a net effect, the determined period will be higher in layers further away from the Ir substrate. It is also assumed that if only the intralayer couplings are considered, then the critical temperature of the layers should increase from the first layer towards the third. The interlayer ferromagnetic couplings J_{12}, J_{23} contribute to the enhancement of the thermal stability, while ensuring that the layers are coupled sufficiently strongly to each other, meaning that the period of the spin spiral will be the same between the three layers at any fixed temperature, and that the triple layer will only have a single critical temperature.

How the period depends on the temperature can be understood from a mean-field model. Following the derivation given in the Supplemental Material [19], the free energy F_{MF} per spin of the spin spiral state with wave vector k may be expressed as

$$\frac{1}{N} F_{\mathrm{MF}}(k) = -\frac{1}{2} \sum_{p,q} \mathcal{J}_{pq}(k) \langle S_p(k) \rangle \langle S_q(k) \rangle$$

$$- \sum_p k_B T \ln \left(4\pi \sinh \left(\frac{B_p(k)}{k_B T} \right) \frac{k_B T}{B_p(k)} \right) \quad (2)$$

with

$$B_p(k) = -\left(\frac{1}{N} \sum_{q,\langle i,j \rangle} J_{pq,ij} \cos \left(k(x_{p,i} - x_{q,j}) \right) \langle S_q(k) \rangle \right.$$

$$\left. + D_{pq,ij} \sin \left(k(x_{p,i} - x_{q,j}) \right) \langle S_q(k) \rangle \right) \quad (3)$$

the mean field in energy dimensions in layer p,

$$\mathcal{J}_{pq}(k) = \frac{1}{N} \sum_{\langle i,j \rangle} J_{pq,ij} \cos \left(k(x_{p,i} - x_{q,j}) \right)$$

$$+ D_{pq,ij} \sin \left(k(x_{p,i} - x_{q,j}) \right) \quad (4)$$

the Fourier transform of the interaction coefficients, and $\langle S_p(k) \rangle$ the order parameter of the spin spiral state. N denotes the number of atoms in a single layer. The equilibrium period of the spin spiral may be obtained by minimizing Eq. (2) with respect to the wave vector k. The wave vector dependence of the free energy is included in the

coupling coefficients $\mathcal{J}_{pq}(k)$, which are minimized by different k values in the different layers as mentioned above. The temperature dependence is encapsulated in the order parameters $\langle S_p(k) \rangle$, which do not depend significantly on the wave vector. However, $\langle S_p(k) \rangle$ decreases faster with temperature in the first and second layers than in the third one, gradually decreasing their relative contribution to the free energy expression (2). This effect shifts the minimum of $F_{\mathrm{MF}}(k)$ towards lower wave vectors with increasing temperature, explaining the effect observed in the experiments.

The interaction coefficients in Eq. (1) were determined based on the above assumptions regarding their relative magnitudes, and the numerical values summarized in Fig. 2(d) were obtained by tuning the values in order to quantitatively reproduce the temperature dependence observed in the experiments by mean-field calculations and Monte Carlo simulations. In particular, the calculations indicated that $|J_{12}| > |J_{23}|$ must be chosen for the interlayer couplings, which was necessary to explain why the period increases faster at higher temperature, by approximately the same factor between 4 and 250 K as between 250 K and room temperature. Figure 2(a) demonstrates a good agreement between the theoretical model and the experiments. The details of the simulations are given in the Supplemental Material [19]. Note that explaining the zigzag wave front of the spin spirals [40] or the range of possible periods at low temperature [28] requires assumptions going beyond the model in Eq. (1), but the Hamiltonian seems to capture the main mechanism behind the temperature dependence of the wavelength.

In summary, we have shown using SP-STM measurements that the observed magnetic period in the triple-layer Fe on Ir(111) increases significantly, by approximately a factor of 16 between 8 and 300 K. Based on the different hybridization and strain relief effects in the three atomic layers, we proposed a theoretical model with layer-dependent coupling coefficients, which quantitatively reproduces the period increase observed in the experiments. Since the presence of different and coupled magnetic layers appears to be decisive, our work shows that the usual mapping of ultrathin films onto a single effective layer might fail to describe temperature effects or phase diagrams for films thicker than a single atomic layer. Our results can hence motivate further investigations in magnetic multilayers regarding the finite temperature behavior of noncollinear spin structures.

*aurore.finco@physnet.uni-hamburg.de

[1] S. S. P. Parkin, M. Hayashi, and L. Thomas, Science **320**, 190 (2008).

[2] A. Fert, V. Cros, and J. Sampaio, Nat. Nanotechnol. **8**, 152 (2013).

[3] I. Dzyaloshinsky, J. Phys. Chem. Solids **4**, 241 (1958).

[4] T. Moriya, Phys. Rev. Lett. **4**, 228 (1960).

[5] C. Moreau-Luchaire, C. Moutafis, N. Reyren, J. Sampaio, C. A. F. Vaz, N. V. Horne, K. Bouzehouane, K. Garcia, C. Deranlot, P. Warnicke, P. Wohlhüter, J.-M. George, M. Weigand, J. Raabe, V. Cros, and A. Fert, Nat. Nanotechnol. **11**, 444 (2016).

[6] G. Chen, A. Mascaraque, A. T. N'Diaye, and A. K. Schmid, Appl. Phys. Lett. **106**, 242404 (2015).

[7] W. Jiang, P. Upadhyaya, W. Zhang, G. Yu, M. B. Jungfleisch, F. Y. Fradin, J. E. Pearson, Y. Tserkovnyak, K. L. Wang, O. Heinonen, S. G. E. te Velthuis, and A. Hoffmann, Science **349**, 283 (2015).

[8] O. Boulle, J. Vogel, H. Yang, S. Pizzini, D. de Souza Chaves, A. Locatelli, T. O. Mente, A. Sala, L. D. Buda-Prejbeanu, O. Klein, M. Belmeguenai, Y. Roussigné, A. Stashkevich, S. M. Chérif, L. Aballe, M. Foerster, M. Chshiev, S. Auffret, I. M. Miron, and G. Gaudin, Nat. Nanotechnol. **11**, 449 (2016).

[9] S. Heinze, K. von Bergmann, M. Menzel, J. Brede, A. Kubetzka, R. Wiesendanger, G. Bihlmayer, and S. Blügel, Nat. Phys. **7**, 713 (2011).

[10] A. Sonntag, J. Hermenau, S. Krause, and R. Wiesendanger, Phys. Rev. Lett. **113**, 077202 (2014).

[11] P. J. Jensen, H. Dreyssé, and K. H. Bennemann, Europhys. Lett. **18**, 463 (1992).

[12] C. M. Schneider, P. Bressler, P. Schuster, J. Kirschner, J. J. de Miguel, and R. Miranda, Phys. Rev. Lett. **64**, 1059 (1990).

[13] H. J. Elmers, J. Hauschild, H. Fritzsche, G. Liu, U. Gradmann, and U. Köhler, Phys. Rev. Lett. **75**, 2031 (1995).

[14] P. Sessi, N. P. Guisinger, J. R. Guest, and M. Bode, Phys. Rev. Lett. **103**, 167201 (2009).

[15] K. von Bergmann, M. Bode, and R. Wiesendanger, J. Magn. Magn. Mater. **305**, 279 (2006).

[16] Y. A. Izyumov, Sov. Phys. Usp. **27**, 845 (1984).

[17] J. Rossat-Mignod, P. Burlet, O. Vogt, and G. H. Lander, J. Phys. C **12**, 1101 (1979).

[18] J. Akimitsu, K. Siratori, G. Shirane, M. Iizumi, and T. Watanabe, J. Phys. Soc. Jpn. **44**, 172 (1978).

[19] See Supplemental Material at http://link.aps.org/supplemental/10.1103/PhysRevLett.119.037202 describing the details of the experiments, the mean-field calculations, and the Monte Carlo simulations, which includes Refs. [20–25].

[20] J. W. Arblaster, Platinum Met. Rev. **54**, 93 (2010).

[21] L. Rózsa, L. Udvardi, L. Szunyogh, and I. A. Szabó, Phys. Rev. B **91**, 144424 (2015).

[22] L. Rózsa, E. Simon, K. Palotás, L. Udvardi, and L. Szunyogh, Phys. Rev. B **93**, 024417 (2016).

[23] L. Szunyogh, L. Udvardi, J. Jackson, U. Nowak, and R. Chantrell, Phys. Rev. B **83**, 024401 (2011).

[24] A. Szilva, M. Costa, A. Bergman, L. Szunyogh, L. Nordström, and O. Eriksson, Phys. Rev. Lett. **111**, 127204 (2013).

[25] D. C. M. Rodrigues, A. Szilva, A. B. Klautau, A. Bergman, O. Eriksson, and C. Etz, Phys. Rev. B **94**, 014413 (2016).

[26] P.-J. Hsu, A. Finco, L. Schmidt, A. Kubetzka, K. von Bergmann, and R. Wiesendanger, Phys. Rev. Lett. **116**, 017201 (2016).

[27] P.-J. Hsu, A. Kubetzka, A. Finco, N. Romming, K. von Bergmann, and R. Wiesendanger, Nat. Nanotechnol. **12**, 123 (2017).

[28] A. Finco, P.-J. Hsu, A. Kubetzka, K. von Bergmann, and R. Wiesendanger, Phys. Rev. B **94**, 214402 (2016).

[29] G. Hasselberg, R. Yanes, D. Hinzke, P. Sessi, M. Bode, L. Szunyogh, and U. Nowak, Phys. Rev. B **91**, 064402 (2015).

[30] Kh. Zakeri, T.-H. Chuang, A. Ernst, L. M. Sandratskii, P. Buczek, H. J. Qin, Y. Zhang, and J. Kirschner, Nat. Nanotechnol. **8**, 853 (2013).

[31] H. L. Meyerheim, J.-M. Tonnerre, L. Sandratskii, H. C. N. Tolentino, M. Przybylski, Y. Gabi, F. Yildiz, X. L. Fu, E. Bontempi, S. Grenier, and J. Kirschner, Phys. Rev. Lett. **103**, 267202 (2009).

[32] Y. Meng, Kh. Zakeri, A. Ernst, T.-H. Chuang, H. J. Qin, Y.-J. Chen, and J. Kirschner, Phys. Rev. B **90**, 174437 (2014).

[33] B. Dupé, G. Bihlmayer, M. Böttcher, S. Blügel, and S. Heinze, Nat. Commun. **7**, 11779 (2016).

[34] O. N. Mryasov, U. Nowak, K. Y. Guslienko, and R. W. Chantrell, Europhys. Lett. **69**, 805 (2005).

[35] S. L. Veber, M. V. Fedin, A. I. Potapov, K. Yu. Maryunina, G. V. Romanenko, R. Z. Sagdeev, V. I. Ovcharenko, D. Goldfarb, and E. G. Bagryanskaya, J. Am. Chem. Soc. **130**, 2444 (2008).

[36] K. von Bergmann, S. Heinze, M. Bode, E. Y. Vedmedenko, G. Bihlmayer, S. Blügel, and R. Wiesendanger, Phys. Rev. Lett. **96**, 167203 (2006).

[37] E. Simon, K. Palotás, B. Ujfalussy, A. Deák, G. M. Stocks, and L. Szunyogh, J. Phys. Condens. Matter **26**, 186001 (2014).

[38] B. Dupé, M. Hoffmann, C. Paillard, and S. Heinze, Nat. Commun. **5**, 4030 (2014).

[39] L. Rózsa, A. Deák, E. Simon, R. Yanes, L. Udvardi, L. Szunyogh, and U. Nowak, Phys. Rev. Lett. **117**, 157205 (2016).

[40] J. Hagemeister, E. Y. Vedmedenko, and R. Wiesendanger, Phys. Rev. B **94**, 104434 (2016).